VERIFICATION OF SOFTWARES FOR ELECTROMAGNETIC FIELD ANALYSIS USING MODELS PROPOSED BY INVESTIGATION COMMITTEES IN IEE OF JAPAN

Norio Takahashi

Department of Electrical and Electronic Engineering, Okayama University
3-1-1 Tsushima, Okayama 700, Japan

Abstract: *In order to investigate methods for analyzing electromagnetic fields and to compare the accuracy and the CPU time of various codes and so on, investigation committees were set up in IEE of Japan. In this paper, the activities of various investigation committees relating electromagnetic field analysis are described from the viewpoint of the verification of software.*

1. INTRODUCTION

In the Institute of Electrical Engineers (IEE) of Japan, twelve investigation committees for analyzing electromagnetic fields have been established from 1977 as shown in Table 1. These committees are composed of 20-30 members from universities, institutes and industries. The committee has a meeting every month or every two months and surveys the following subjects, for example:

(1) recently developed methods for calculating electromagnetic fields,
(2) validity of newly developed methods,
(3) new application areas of numerical analysis of electromagnetic fields.

Some committees have proposed models in order to verify various numerical methods. Each committee published an IEEJ Technical Report.

In this paper, verification models proposed by the committees of IEE of Japan and some results reported by committee members are shown. Results of calculation of magnetic fields, eddy currents, forces, torques, optimized shapes and measurement carried out by the author are also

Table 1 Investigation committees in IEE of Japan

no.	period *	name	number of members		
			univ.	inst.	indust.
1	1977 - 1980	Investigation Committee on Electromagnetic Field Analysis of Electric Power Machines Using Finite Element Method	8	1	10
2	1980 - 1984	Investigation Committee on Applications of Numerical Method for Analyzing Electric Power Machines	11	2	12
3	1984 - 1987	Investigation Committee on 3-D Calculation of Electromagnetic Fields	12	2	10
4	1987 - 1990	Investigation Committee on Numerical Analysis of Eddy Current	10	1	14
5		Investigation Committee on Applications of Numerical Method for Analyzing Magnetic Fields in Rotating Machines	14	0	12
6	1990 - 1993	Investigation Committee on Techniques for Applications of 3-D Electromagnetic Field Analysis	12	1	17
7		Investigation Committee on Software for Numerical Analysis of Magnetic Fields in Rotating Machines	10	0	14
8	1993 - 1995	Investigation Committee on Highly Accurate Simulation Technique for Rotating Machines	8	0	17
9	1993 - 1996	Investigation Committee on Electromagnetic Field Analysis and Its Applications to Optimization Problems	11	3	14
10	1995 - 1997	Investigation Committee on Techniques for Applications of Electromagnetic Field Analysis for Rotating Machines	10	0	16
11	1996 - 1999	Investigation Committee on Highly Advanced Optimization Technique for Electromagnetic Problems	13	2	16
12	1997 - 1999	Investigation Committee on Techniques of Electromagnetic Field Analysis for Virtual Engineering of Rotating Machines	8	0	17

* : The committees start in April and end in March.

discussed.

2. MAGNETOSTATIC AND EDDY CURRENT MODELS (1984-1990)

A. 1984-1987

The "Investigation Committee on 3-D Calculation of Electromagnetic Fields" (1984-1987, Chairman: T. Nakata, Okayama Univ.) proposed a simple 3-D magnetostatic model[1] as shown in Fig.1, so that many universities, institutes and industries can join the project. The rectangular open core is surrounded by a d.c. exciting winding with 457 turns. The d.c. current is equal to 6.56A. A magnetic shield box of which the thickness t is 1.6mm covers the model. The relative permeabilities of the core and the shield are assumed to be 1000.

Fig.2 shows the calculated flux distribution. Fig.3 shows the absolute value of flux density above the core (z=110mm). Fig.4 shows the effects of the thickness t and the relative permeability μs of the shield box on the flux density at the point of x=y=0, z=110mm. When t is increased, the flux density is not changed with t. The change of flux density by the thickness t is small when μs is increased. The effect of the gauge condition of the $\boldsymbol{A}$-method on the obtained result is discussed[3]. The cancellation error of the T-W method[4] and the error of the boundary element method[5] are discussed.

B. 1987-1990

The "Investigation Committee on Numerical analysis of Eddy Current" (1987-1990, Chairman: T. Onuki, Waseda Univ.) proposed a 3-D eddy current model[6] as shown in Fig.5. A rectangular ferrite core is surrounded by an exciting coil. An ac current of which the effective value is 1000AT at the frequency of 50Hz is applied. Two aluminum plates are set on the upper and lower sides of the core. The conductivity of the aluminum is equal to 3.215×10^7 S/m, and the relative permeability (μr) of the core is assumed to be 3000. Both cases with and without a hole in the plate are investigated.

Magnetic field noise is induced at the junction of the Hall sensor and lead wires, and this noise cannot be easily eliminated by simply twisting the lead wires. Therefore, the flux density is measured using a small search coil

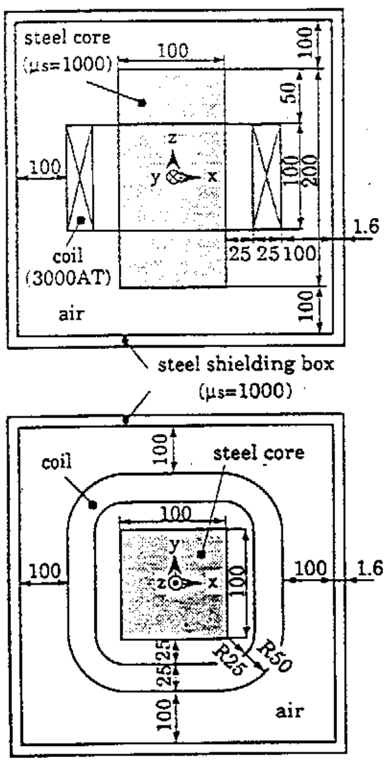

Fig.1 3-D Magnetostatic model.

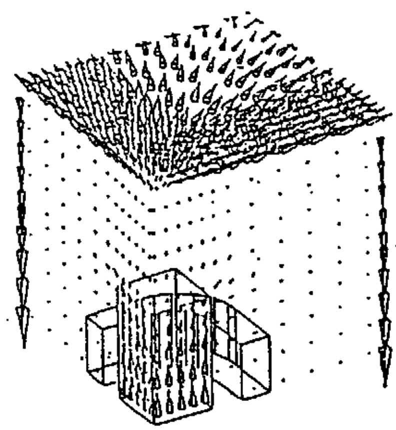

(a) bird's-eye view

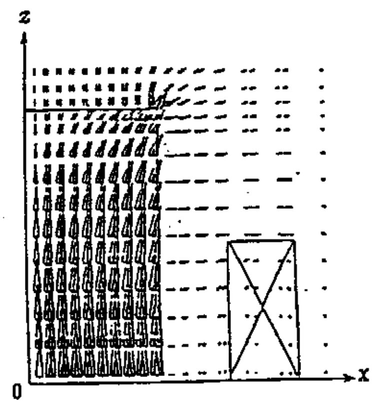

(b) cross section(y=0mm)

Fig.2 Flux distribution.

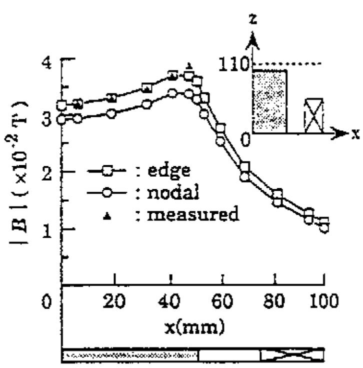

Fig.3 Spatial distribution of flux density (with shield, y=47mm, z=110mm).

with 20 turns (mean diameter: 3mm, height: 0.6mm, conductor diameter: 0.06mm). The eddy current density on the surface of the aluminum plate is measured using a modified probe method[26], and the total eddy current is measured using a Rogowski coil.

Fig.6 shows the distributions of flux density vectors. Fig.7 shows the maximum absolute value $|\mathbf{B}|$ of the flux density along the line at z=57.5mm[7]. The discrepancies between the calculated and measured values are quite small. Fig.8 shows the distributions of eddy current density vectors. Fig.9 shows the x- and y-components of the maximum value of the eddy current density on the surface (z=65mm) of the aluminum plate. The results calculated using various methods and elements are almost the same. The discrepancies between the calculated and

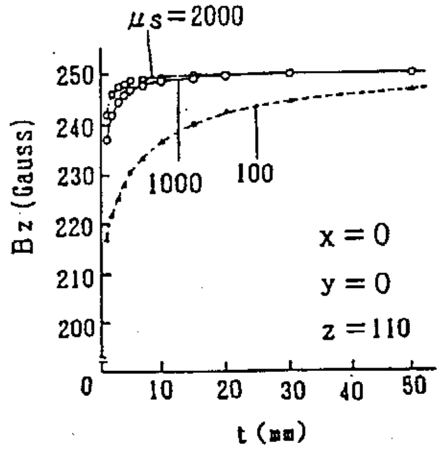

Fig.4 Effect of thickness t on flux density.

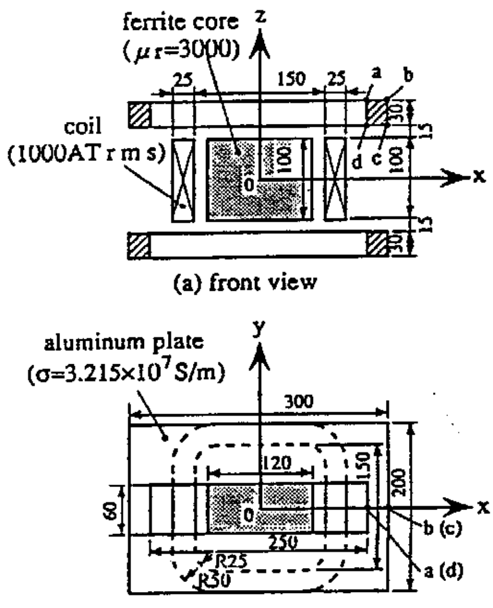

(a) front view

(b) plan view

Fig.5 3-D eddy current model.

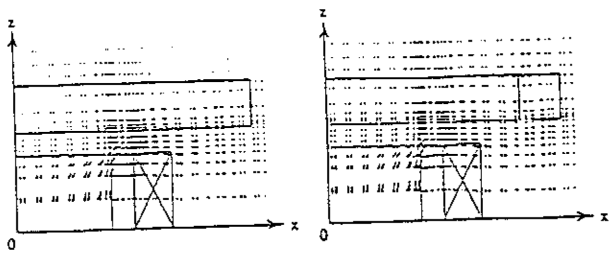
(a) without hole (b) with hole

Fig.6 Distributions of flux density vectors (y=0mm, ωt=0°).

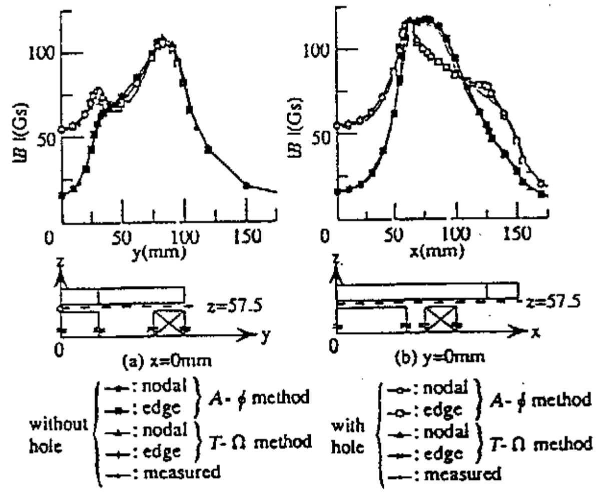

Fig.7 Distributions of flux density (z=57.5mm).

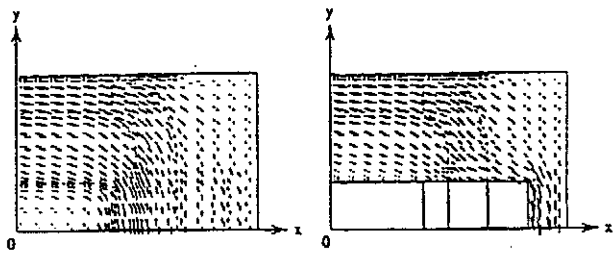
(a) without hole (b) with hole

Fig.8 Distributions of eddy current density vectors (z=65mm, ωt=0°).

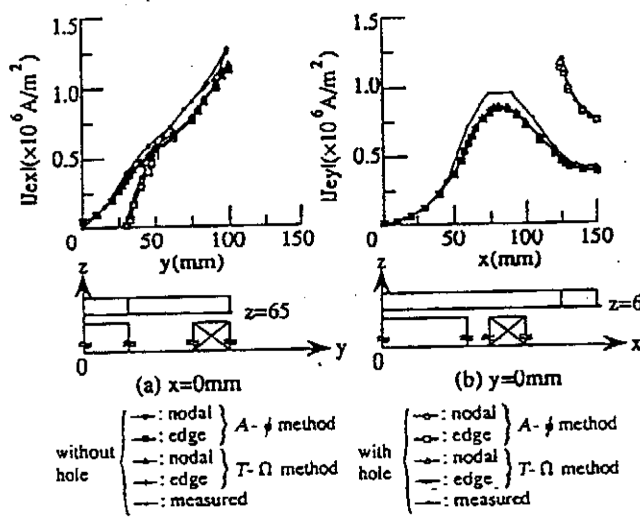

Fig.9 Distribution of eddy current density (z=65mm).

measured values may be due to an insufficient number of elements, setting error of sensor, etc. Table 2 shows the comparison of calculated and measured values of total eddy current I_e passing through the cross section a-b-c-d-a in Fig.5. The error ε is defined by

$$\varepsilon = \left| \frac{Ie\,(cal) - Ie\,(mea)}{Ie\,(mea)} \right| \times 100\% \qquad (1)$$

where I_e (cal) is the current calculated and I_e (mea) is the current measured.

The number of iterations of ICCG (Incomplete Cholesky Conjugate Gradient) method for calculating large simultaneous equations, the CPU time, etc. are shown in Table 3. The CPU time of the **T**-Ω method in the analysis of the model without hole decreases considerably compared with the A-φ method. The CPU times of the edge element for the *A*-φ and **T**-Ω methods are about 1/6 and 1/2 of the nodal element. Although the CPU time of the **T**-Ω method in the analysis of the model with hole is much larger compared with that without hole in the case of nodal element, it is not so remarkable in the case of edge element. From the viewpoints of the CPU time, the **T**-Ω method with edge element is favorable.

A new formulation of the *A*-φ method[8], a hybrid FE-BE method[9], the boundary element method using edge elements[10] and the finite element method with integral equation[11] are discussed.

3. MODELS FOR CALCULATING FORCE AND TORQUE (1990-1995)

A. 1990-1993

The "Investigation Committee on Software for Numerical Analysis of Magnetic Fields in Rotating Machines" (1990-1993, Chairman: T. Nakata, Okayama Univ.) proposed four kinds of models which are related to magnetic field analysis of rotating machines[12].

Fig.10 shows a 3-D model for the verification of dc force calculation[13,14]. The center pole and yoke are made of steel. The coil has 381 turns and the ampere-turns (dc) are chosen to be 1000, 3000, 4500 and 5000 in order to investigate the saturation effect. Fig.11 shows the z-component F_z of electromagnetic force calculated using the Maxwell stress tensor method, advanced energy method and magnetizing current method. The number of elements, n_e, is equal to 108864. The force calculated by the Maxwell stress tensor method using the edge element with **A** (magnetic vector potential) variable is the nearest to the measured value. The rate of increase of the force with current is reduced above 3000AT due to the saturation of the center pole.

Fig.12 shows the effect of number of elements, n_e, on the results calculated. Fig.13 shows the initial mesh (n_e=4032). Each side of individual elements is subdivided into twice (n_e=4032 × 2^3=32256) and thrice (n_e=4032 × 3^3=108864). The figure suggests that the force calculated by the Maxwell stress tensor method

Table 2 Comparison of eddy current (with hole)

item	$A-\phi$		$T-\Omega$		measured
	nodal	edge	nodal	edge	
amplitude of eddy current $\|I_e\|$ (A)	449	451	450	450	444
error ε_3 (%)	1.13	1.58	1.35	1.35	——

Table 3 Discretization data and CPU time

item	without hole				with hole			
	$A-\phi$		$T-\Omega$		$A-\phi$		$T-\Omega$	
	nodal	edge	nodal	edge	nodal	edge	nodal	edge
number of elements	14400							
number of nodes	16275							
number of unknowns	43417	41060	22844	22412	42885	41060	22844	22412
number of non-zero entries	1781644	653718	632859	423056	1734684	653718	632859	423056
computer storage (MB)	72.2	28.4	30.7	19.4	70.5	28.4	30.7	19.4
number of iterations of ICCG method	1306	513	172	192	1264	582	1141	327
CPU time (s)	6242	947	533	290	5870	1069	2001	442

Computer used : NEC supercomputer SX-1E
(maximum speed : 285 MFLOPS)

convergence criterion of ICCG method : 10^{-7}

using the magnetic vector potential (A) converges to a constant value when n_e is nearly equal to 30000. On the contrary, the forces calculated by the advanced energy method and the magnetizing current method change with n_e. It is difficult to make a mesh which has extremely dense and sparse parts, unless the nonconforming element[8] is used. That is the reason why the convergence characteristic is so poor in Fig.12.

Fig.14 shows the 2-D model for verification of the torque calculation[15]. The stator core is made of non-oriented silicon steel (AISI: M-36). The rotor is composed of 4 poles. The rotor shaft is made of carbon steel. The rotor magnets are made of $SmCo_5$ (B_r=0.9T, H_c=7.0 × 10^6 A/m), and magnetized in parallel. Twelve participants solved the cogging torque and seven groups measured it.

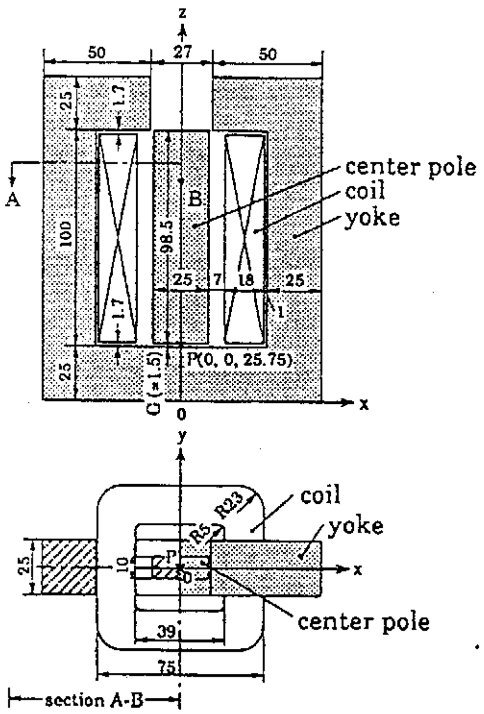

Fig.10 3-D model for verification of force calculation.

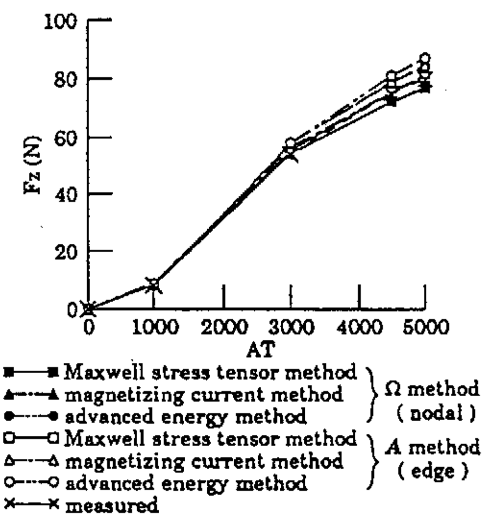

Fig.11 z-component Fz of electromagnetic force.

Fig.15 shows the waveforms of cogging torque calculated by twelve (A-L) participants. The maximum and minimum waveforms of calculated cogging torque and measured waveform are compared in Fig.16. The 2-D finite element method using 1st order triangular elements

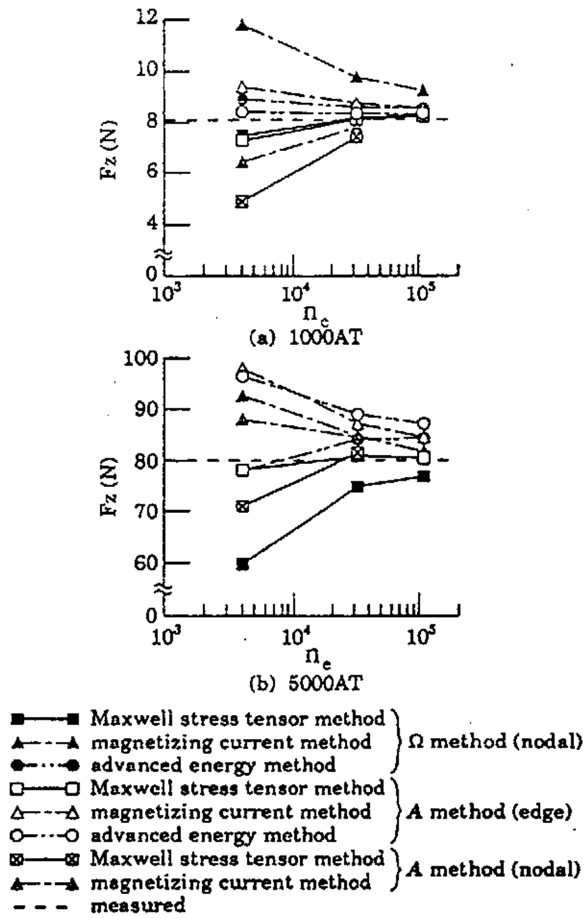

Fig.12 Effect of number of elements n_e.

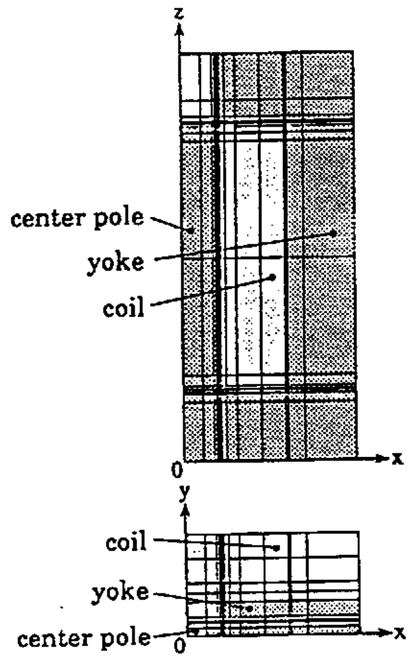

Fig.13 Initial mesh (ne=4032).

is used. The cogging torque, T, is calculated using the Maxwell stress tensor method and the advanced energy method. In order to obtain the cogging torque as a function of rotor angular displacement, numerical field solutions are obtained for different rotor positions.

The torque is calculated for two kinds of mesh patterns as shown in Fig.17. Fig.18 shows the effect of the mesh pattern on the torque calculated. The figure suggests that the results obtained by the Maxwell stress tensor method are affected by the mesh pattern. On the contrary, the results obtained by the advanced energy method are scarcely affected by the mesh pattern. Fig.19 shows the effect of the position of integration path in the air gap of the Maxwell stress tensor method on the calculated cogging torque under no load. The result obtained for the fine mesh (n_e=17352) and the measured result are also shown. The figure suggests that the accuracy of the result for the integration path along the middle contour (r=11.75mm, r: radius from the center of rotor shaft) in the air gap and that along the rotor side contour (r=11.55mm) are better than that along the stator side contour (r=11.95mm). This is because the change of the flux distribution is significant near the teeth of the stator.

The cogging torque calculated using 3-D analysis is compared with that using 2-D analysis[16]. It is shown that the result of 3-D analysis is a little closer to the measured result.

Fig.20 shows a linear motor model[12]. The field is composed of yoke (steel) and 2 pole ferrite magnets. The armature core is made of steel. The number of turns of each winding is 50. Fig.21 shows the comparison of calculated and measured thrust and attractive forces.

Fig.22 shows a model of salient-pole synchronous machine[12]. The number of poles is 6. The core is made of non-oriented silicon steel (AISI: M-47). Fig.23 shows the calculated flux distributions in the air gap.

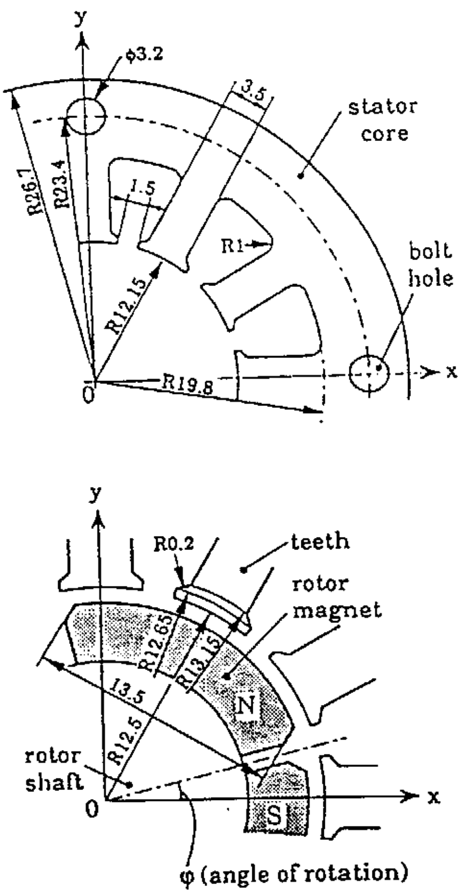

Fig.14 2-D model for verification of torque calculation.

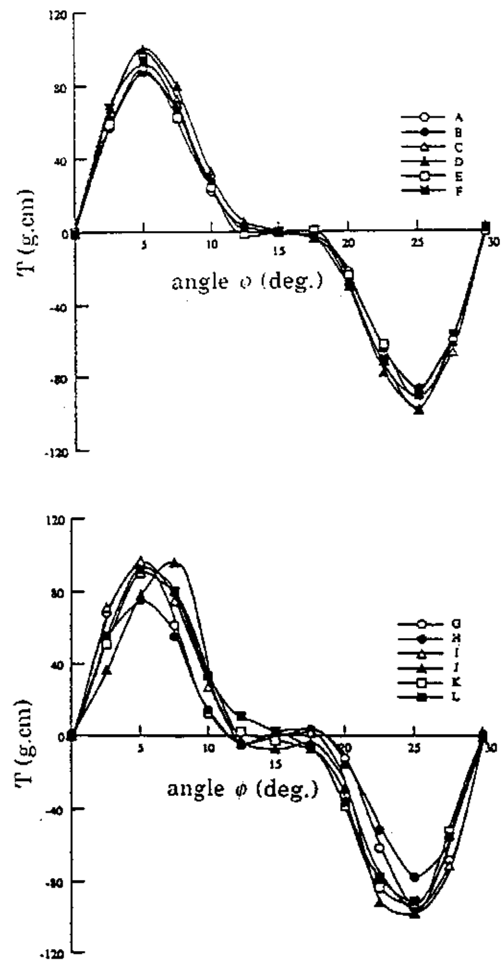

Fig.15 Cogging torques calculated by twelve participants.

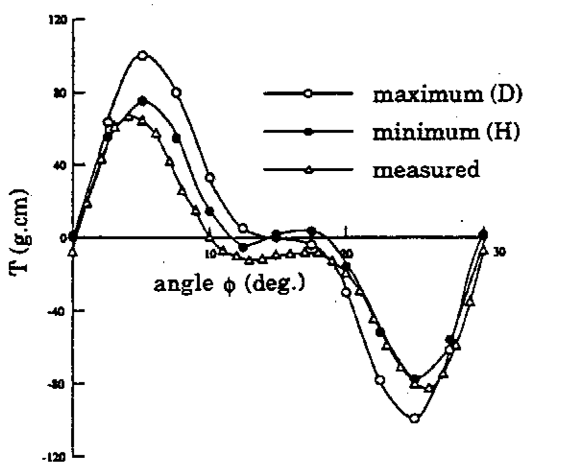

Fig.16 Maximum and minimum calculated cogging torques and measured one.

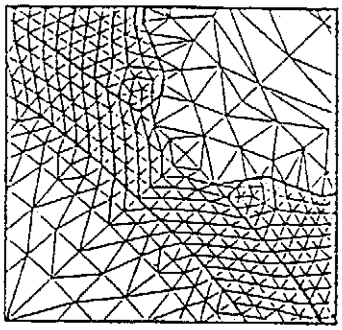

(a) mesh-1

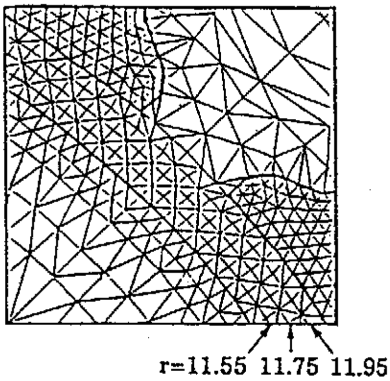

(b) mesh-2

Fig.17 Mesh in and around gap (n_e=4338).

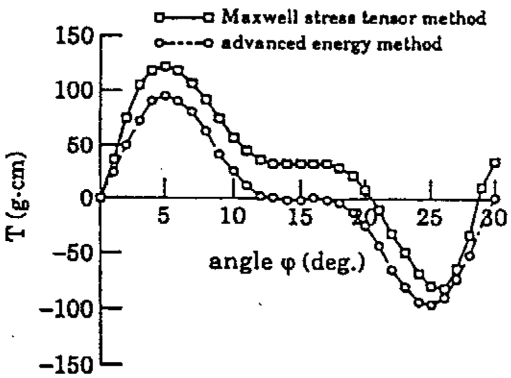

(a) mesh-1

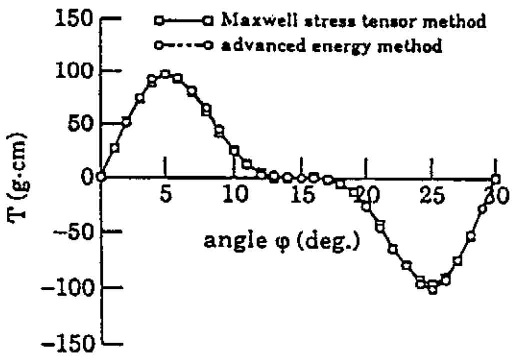

(b) mesh-2

Fig.18 Effect of subdivision in air gap.

B. 1993-1995

In the "Investigation Committee on Highly Accurate Simulation Technique for Rotating Machines" (1993-1995, Chairman: M. Itoh, Hitach Ltd.), the torque under load and the load current, etc. of the permanent magnet motor model shown in Fig.14 are analyzed[17]. Fig.24 shows the connection of stator windings. Fig.25 shows the torque-speed characteristics[18]. Torques under various excitation conditions are analyzed[19,20].

4. MODELS FOR COMPARING OPTIMIZATION METHODS (1993-1996)

The "Investigation Committee on Electromagnetic Field Analysis and Its Application to Optimization Problems" (1993-1996, Chairman: T. Takuma, Kyoto Univ.) proposed five kinds of models for the comparison of optimization methods[21].

Fig.26 shows a model of die press with electromagnet for orientation of magnetic powder[22]. This is used for producing anisotropic permanent magnets. The die press is made of steel. The die molds are set to form the radial

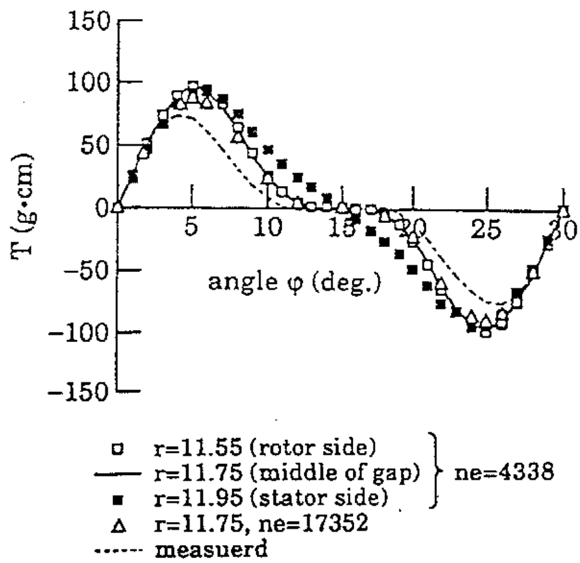

Fig.19 Cogging torque.

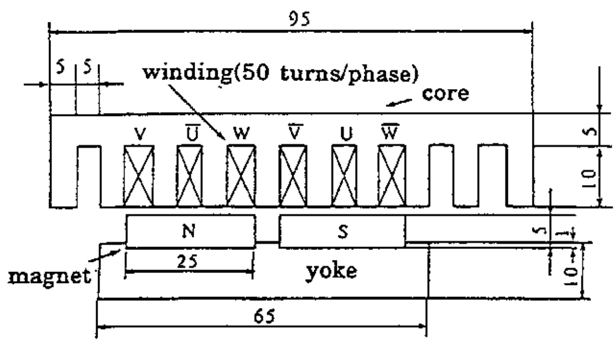

Fig.20 Linear motor model.

flux distribution. The magnetic powder is inserted in the cavity. The ampere-turns of each coil are 33.7kAT. x- and y-components B_x and B_y of flux density at the points along the line e-f in the cavity are specified as follows:

$$\left.\begin{aligned} Bx &= 1.5\cos\theta(T) \\ By &= 1.5\sin\theta(T) \end{aligned}\right\} \qquad (2)$$

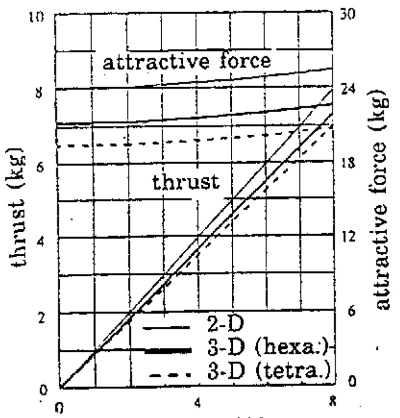

(a) calculated

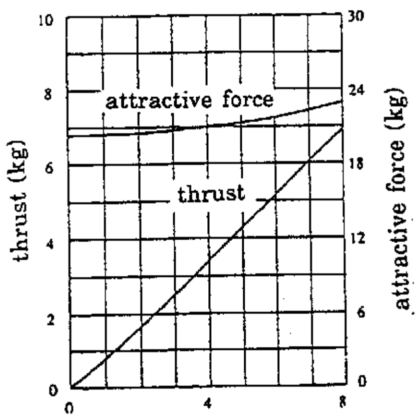

(b) measured

Fig.21 Thrust and attractive force.

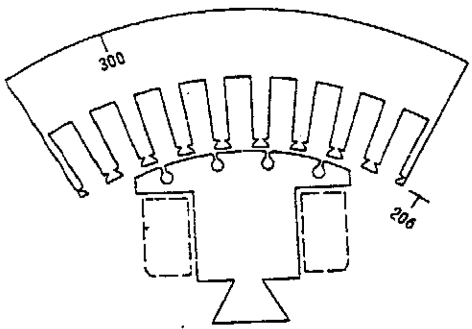

minimum gap : 1.3mm
thickness of core : 100mm

Fig.22 Synchronous machine model

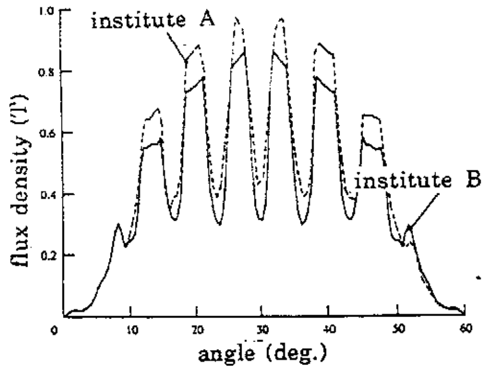

Fig.23 Flux distribution along air gap (1300AT).

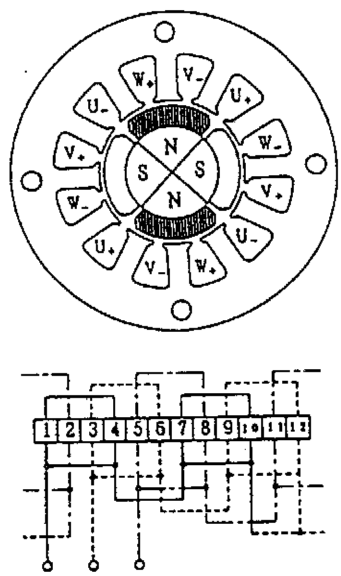

Fig.24 Connection of stator winding.

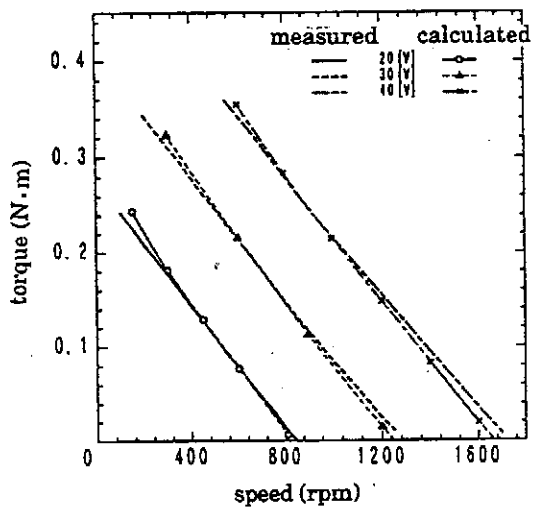

Fig.25 Torque-speed characteristics.

where θ is the angle measured from the x-axis. The following four kinds of optimization methods are applied to this model.

(a) Physical and Engineering Investigation Method (PEM)
The shape of the magnetic circuit is examined from the physical and engineering viewpoint (Fig.27(a)). Finally four kinds of design variables (r_1-r_4) are chosen as shown in Fig.27 (b) and the final result using the simulated annealing method is shown in Fig.27(c).

(b) Genetic Algorithm Method (GAM)
Fig.28 (a) shows the initial shape. The points 1-6 are moved in the radial direction, whereas the points 7-12 are moved in the x-direction. 4 bits are specified for each GA node. Fig.28 (b) shows the final shape obtained after 190 generations.

(c) Rosenbrock's Method (RBM) and Simulated Annealing Method (SAM)
Fig.29 (a) denotes the definition of design variables. n-p and k-m are denoted by ellipses whose long and short axes are L1, L2, L3 and L4. Fig.29 (b) shows the final shapes obtained using RBM and SAM.

Fig. 30 shows the comparison of the amplitude and direction of the flux density vector which are obtained using four kinds of methods. The advantage and disadvantage of each method should be investigated in the future.

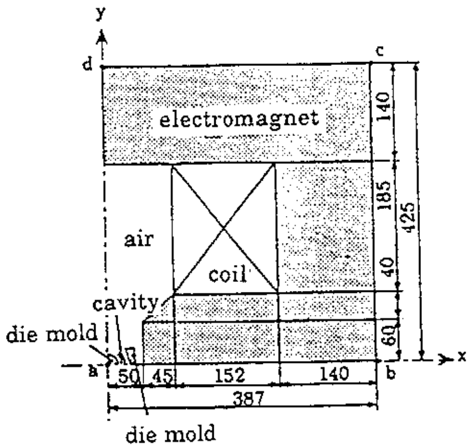

a-b-c-d: Dirichlet boundary
d-a: Neumann boundary

(a) whole view

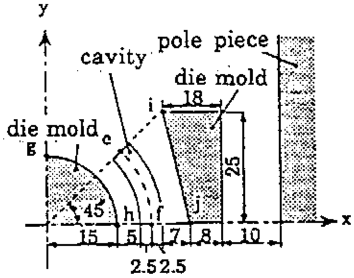

(b) enlarged view

Fig.26 Model of die press with electromagnet.

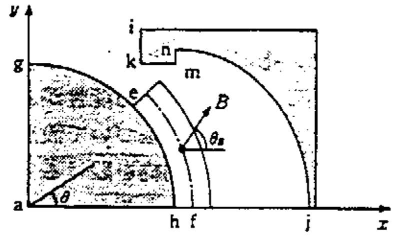

(a) investigation of shape of magnetic circuit

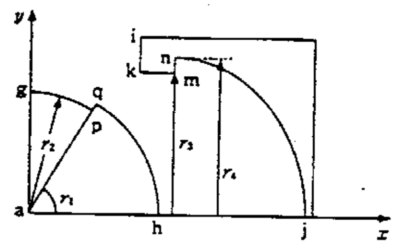

(b) choice of design variables

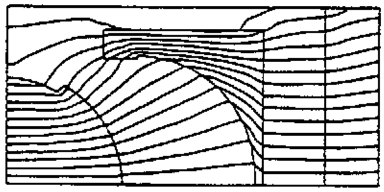

(c) final shape

Fig.27 Optimization by physical and engineering investigation method (PEM).

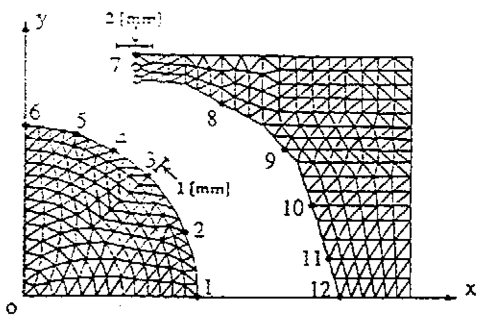

(a) points to be moved

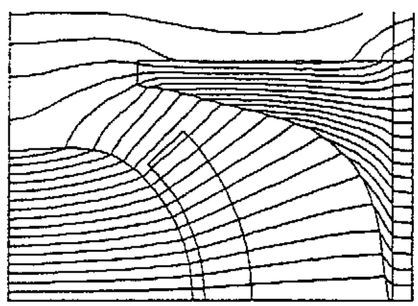

(b) final shape

Fig.28 Optimization by genetic algorithm (GA).

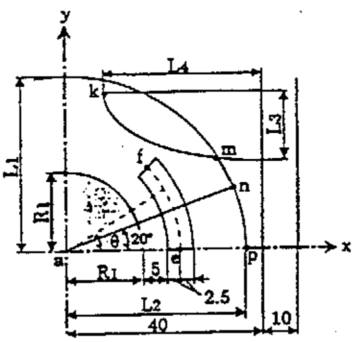

(a) definition of design variables

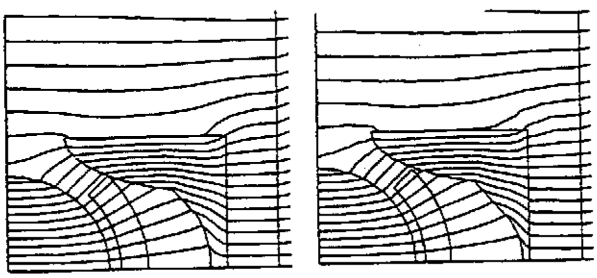

RBM SAM

(b) final shapes

Fig.29 Optimization by Rosenbrock's method (RBM) and simulated annealing method (SAM).

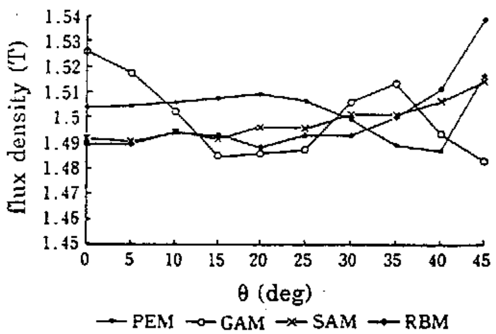

(a) flux density

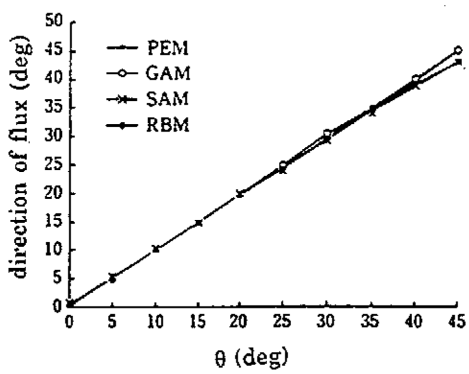

(b) direction of flux

Fig.30 Flux density and direction of flux at final shape.

Fig.31 shows a superconducting MRI magnet model[21]. The uniform flux density is 1.5T. The required uniformity in the center sphere (radius: 200mm) is less than 5ppm. Fig.32 shows the obtained result using the quasi-Newton method and theoretical equation of magnetic field[23]. The obtained uniformity is 0.4ppm.

Fig.33 shows the axi-symmetric electrode model[21]. Fig.34 shows the obtained shape of the electrode which

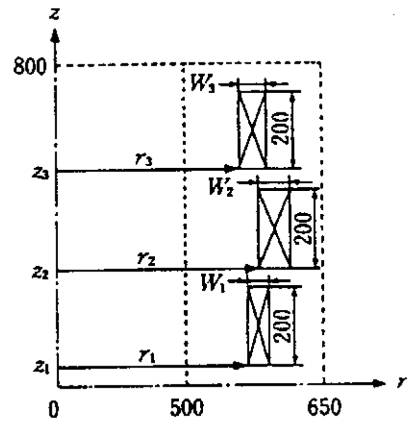

Fig.31 MRI magnet model.

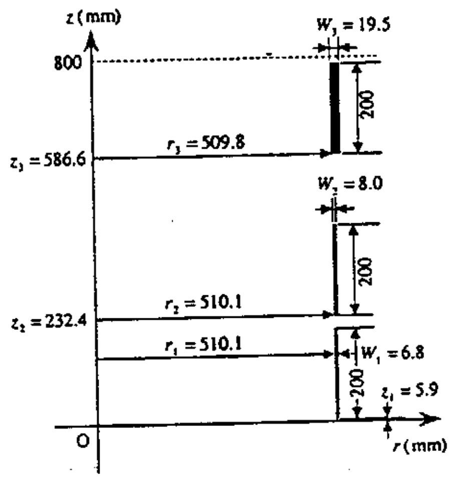

Fig.32 Optimal configuration.

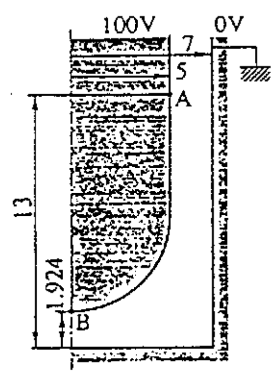

Fig.33 Axi-symmetric electrode model.

produces the uniform electric field intensity[24]. The electric field is calculated using the charge simulation method (CSM) and the surface charge method (SCM).

Fig.35 shows the sphere electrode in a cube[21]. Fig.36 shows the obtained shape of the electrode which produces the uniform electric field intensity[24].

Fig.37 shows the 3-D shielding model[21]. The ferrite plate has the relative permeability of 1000 and is energized by 39789AT. Fig.38 shows the obtained shape of the plate having various partial thickness so that the maximum value of the flux density in the observation area is less than 0.005T.

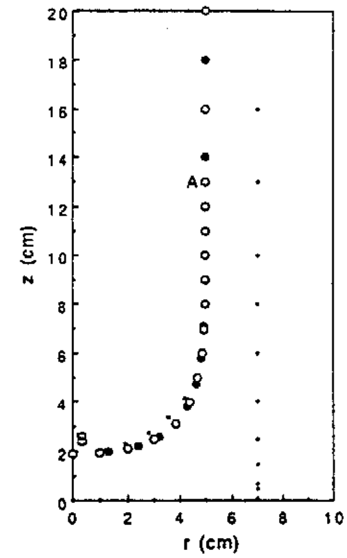

Fig.34 Obtained shape of axi-symmetric electrode.

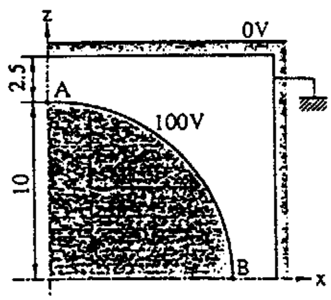

Fig.35 Sphere electrode model.

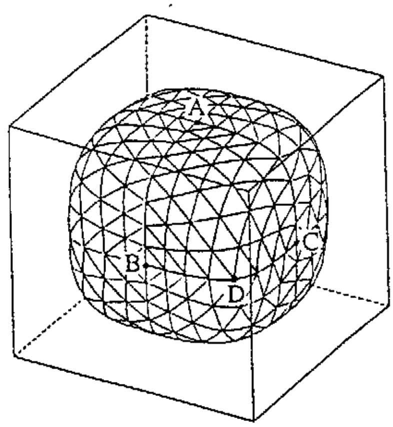

Fig.36 Obtained shape of 3-D electrode.

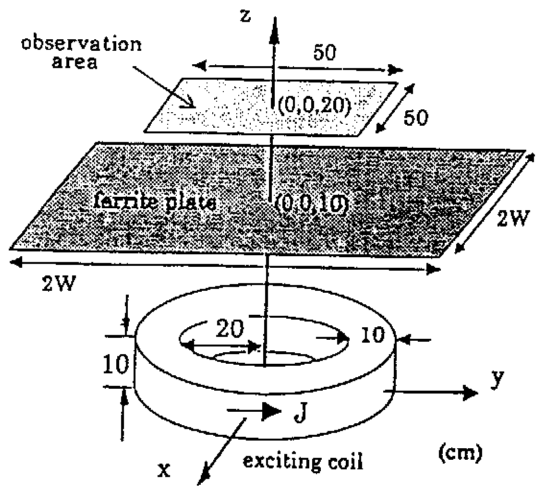

Fig.37 3-D magnetic shield model.

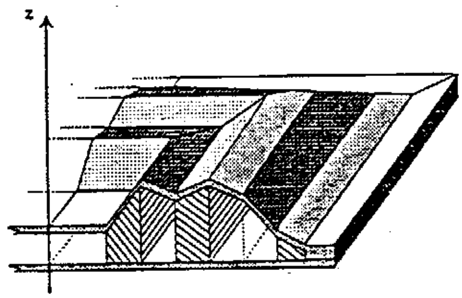

Fig.38 Obtained plate shape.

5. CONCLUSIONS

The verification models proposed by the investigation committees of IEE of Japan and some results are discussed. Various knowledge related to electromagnetic field calculation was obtained by using these models. The detailed discussion is written in each paper. Some models (Fig.10 and the modified version of Fig.26) were also adopted as TEAM Workshop problems (Problems 20 and 25[25]).

The verification of the following problems should be investigated in the future:
(a) modeling of material properties, such as anisotropy, hysteresis and superconductivity,
(b) coupled problems with heat and fluid flow,
(c) optimization method of actual machines.

I think such activities of the verification of softwares using various models shown in this paper made considerable contribution to the progress of the electromagnetic field calculation in Japan.

REFERENCES

[1] IEEJ Technical Report, no.286, "Numerical technique for analyzing 3-D magnetostatic field", 1988.

[2] T. Nakata, N. Takahashi and K. Fujiwara, "3-D finite element analysis of magnetic fields of IEEJ model", *Electromagnetic Fields in Electrical Engineering*, pp.285-288, Pergamon Press, 1988.
[3] Y. Kanai, T. Abe, M. Sengoku, T. Iijima, M. Iizuka and K. Mukasa, "Further discussion on magnetic vector potential finite-element formulation for three-dimensional magnetostatic field analysis," IEEE Trans. on Magnetics, vol.26, no.2, pp.411-414, 1990.
[4] T. Nakata, N. Takahashi, K. Fujiwara and T. Imai, "Effects of permeability of magnetic materials on errors of the T-W method," IEEE Trans. on Magnetics, vol.26, no.2, pp.698-701, 1990.
[5] K. Sawa and T. Hirano, "An evaluation of the computational error near the boundary with magnetostatic field calculation by B.E.M.," IEEE Trans. on Magnetics, vol.26, no.2, pp.403-406, 1990.
[6] IEEJ Technical Report, no.384, "Numerical technique for analyzing 3-D eddy current", 1991.
[7] T. Nakata, N. Takahashi, K. Fujiwara, T. Imai and K. Muramatsu, "Comparison of various methods of analysis and finite elements in 3-D magnetic field analysis", IEEE Trans. on Magnetics, vol.27, no.5, pp.4073-4076, 1991.
[8] P. Robert, M. Ito and T. Takahashi, "Numerical solution of three dimensional transient eddy current problems by the A-f method," IEEE Trans. on Magnetics, vol.28, no.2, pp.1166-1169, 1992.
[9] T. Onuki and S. Wakao, "Novel boundary element formulation in hybrid FE-BE method for electromagnetic field computations," IEEE Trans. on Magnetics, vol.28, no.2, pp.1162-1165, 1992.
[10] T. Onuki and S. Wakao, "Novel boundary element analysis for 3-D eddy current problems," IEEE Trans. on Magnetics, vol.29, no.2, pp.1520-1523, 1993.
[11] Y. Tanaka, "Three-dimensional eddy current analysis by the finite element method with integral equations using T-Ω," IEEE Trans. on Magnetics, vol.28, no.2, pp.1150-1153, 1992.
[12] IEEJ Technical Report, no.486, "Software for numerical analysis of magnetic fields in rotating machines", 1994.
[13] T. Nakata, N. Takahashi, Suhartono and H. Morishige, "Investigation of a model to verify softwares for 3-D static force calculation", IEEE Trans. on Magnetics, vol.30, no.5, pp.3483-3486, 1994.
[14] T. Nakata and N. Takahashi, "Verification of 3-D software for calculating electromagnetic force", Electromagnetic Field Problems and Applications, International Academic Publishers, pp.7-10, 1993.
[15] N.Takahashi, T.Nakata and H.Morishige, "Verification of software for calculating electromagnetic force and torque using IEEJ model", Software Applications in Electrical Engineering, pp.221-227, Computational Mechanics Publications, 1993.
[16] Y. Kawase, T. Yamaguchi and Y. Hayashi, "Analysis of cogging torque of permanent magnet motor by 3-D finite element method," IEEE Trans. on Magnetics, vol.31, no.3, pp.2044-2047, 1995.
[17] IEEJ Technical Report, no.565, "Highly accurate simulation technique for rotating machines", 1995.
[18] N. Igura, T. Shimomura, K. Harada, Y. Ishihara and T. Todaka, "A proposal for rotating machineries analysis by considering the unknown equal potential condition on FEM," IEEE Trans. on Magnetics, vol.31, no.3, pp.1722-1724, 1995.
[19] Y. Kawase, Y. Hayashi, T. Yamaguchi, Y. Ishihara and Y. Kitamura, "3-D finite element analysis of permanent-magnet motor excited from square pulse voltage source," IEEE Trans. on Magnetics, vol.32, no.3, pp.1537-1540, 1996.
[20] T. Yamaguchi, Y. Kawase and Y. Hayashi "Dynamic transient analysis of vector controlled motors using 3-D finite element method," IEEE Trans. on Magnetics, vol.32, no.3, pp.1549-1552, 1996.
[21] IEEJ Technical Report, no.611, "Electromagnetic field analysis and its application to optimization problems", 1996.
[22] N. Takahashi, K. Ebihara, K. Yoshida, T. Nakata, K. Ohashi and K. Miyata, "Investigation of simulated annealing method and its application to optimal design of die mold for orientation of magnetic powder", IEEE Trans. on Magnetics, vol.32, no.3, pp.1210-1213, 1996.
[23] M. Kitamura, S. Kakukawa, K. Mori and T. Tominaka, "An optimal design technique for coil configurations in iron-shielded MRI magnets," IEEE Trans. on Magnetics, vol.30, no.4, pp.2352-2355, 1994.
[24] H.Tsuboi and T.Misaki, "Optimization of electrode and insulator contours by using Newton method", Trans. of IEE of Japan, vol.106, no.7, pp.307-314, 1986.
[25] Proceedings of the TEAM Workshop in the Sixth Round, Okayama, 1996.
[26] T.Nakata, K.Fujiwara, M.Nakano and T.Kayada, "Effects of construction of yokes on the accuracy of a single sheet tester", Anales de Fisica, Serie B, vol.86, pp.190-192, 1990.